

Solid state reaction of ruthenium with 6H-SiC under vacuum annealing and the impact on the electrical performance of its Schottky contact for high temperature operating SiC-based diodes

Kinnock V. Munthali,^{1,2} Chris Theron¹, F. Danie Auret¹, Sergio M.M. Coelho¹, Linda Prinsloo¹, Eric Njoroge¹

¹Department of Physics, University of Pretoria, Pretoria 0002, South Africa
Phone: +27 124204777
Fax: +27 123625288
Email: kvmunthali@gmail.com

² Department of Mathematics, Science and Sports Education, University of Namibia; HP Campus, P/Bag 5507, Oshakati, Namibia

Abstract

Thin films and Schottky diodes dots of ruthenium (Ru) on bulk-grown n-type-6-hexagonal-silicon carbide (6H-SiC) were annealed isochronally in a vacuum furnace at temperatures ranging from 500 -1000 °C. Rutherford backscattering spectroscopy analysis of the thin films showed formation of ruthenium silicide (Ru₂Si₃) at 800 °C, while diffusion of Ru into 6H-SiC commenced at 800 °C. Raman analysis of the thin films annealed at 1000 °C showed clear D and G carbon peaks which was evidence of formation of graphite. At this annealing temperature the Schottky contact was observed to convert to an ohmic contact, as evidenced by the linearity of current-voltage characteristic, thereby rendering the diode unusable. The transformation from Schottky contact to ohmic contact is attributed to graphite formation at the interface.

Keywords

Rutherford backscattering spectrometry, Raman spectroscopy, ruthenium, graphite, ruthenium silicide, 6H-SiC, D and G carbon peaks, Schottky contacts.

1. Introduction

Silicon carbide (SiC) is used in both microelectronics and tristructural isotropic (TRISO) coated fuel particles in high temperature nuclear reactors. Its properties of large bandgap, high breakdown electric field, high thermal conductivity, high saturation carrier velocity [1], find applications in high temperature operating electronic devices. Ruthenium (Ru) has a high melting point (2250° C), high chemical stability, low electrical resistance, high mechanical resistance to abrasion and fatigue [2]. These properties make Ru a good candidate as a schottky contact for high temperature operating schottky barrier diodes. The stability of Ru contact with 6-hexagonal-silicon carbide (6H-SiC) at high temperatures is indispensable for electronic device integrity. It is therefore important to study how the reaction and diffusion of ruthenium with SiC, affects the performance of Ru-6H-SiC diodes. However there is scant literature [3,

4,5,6,7,8,9] on the solid state reaction of Ru with SiC, and its effect on the performance of Ru-on-SiC based diodes .

2. Experimental Method

Bulk-grown n-type 6H-SiC samples from Cree Research were prepared for metallization by degreasing, using an ultra-sonic bath for a period of 5 minutes for each step, in trichloroethylene, acetone, methanol and deoxidizing 10% HF and then rinsed in deionised water. The samples were finally dried with nitrogen before loading them into the vacuum chamber where 50 nm film of Ru was deposited by e-beam at 10^{-6} mbar pressure. The Ru film thickness was monitored by Inficon meter until the required thickness was obtained. The 6H-SiC used for making Schottky dots was cleaned as explained above before loading it in a vacuum chamber where 200nm of nickel (Ni) was deposited on the rough surface of 6H-SiC by vacuum resistive evaporation at a pressure of 10^{-5} mbar. After nickel deposition, the sample was annealed in an argon atmosphere in a Lindberg Heviduty furnace at a temperature of 1000°C for 1 minute to make the nickel contact ohmic. The annealed sample was then chemically cleaned again in trichloroethylene, acetone and methanol, and deionised water before a 50nm thick of Ru was deposited on the polished side (Si-face) of the sample by an electron-beam deposition technique through a metal contact mask at 10^{-6} mbar pressure. Both the Schottky diodes and thin film samples were simultaneously annealed in a vacuum furnace at pressures of less than 10^{-7} mbar for a period of 1 hour for temperatures ranging from 500 °C to 1000 °C. After each annealing temperature Rutherford backscattering spectroscopy (RBS) was used to analyse the thin film samples. RBS uses a beam of monoenergetic (usually α , $^4\text{He}^+$ and $^1\text{He}^+$) particles produced in an accelerator which bombard the sample to be investigated. Some of the projectiles will undergo close collisions with the nuclei of single atoms, and get backscattered. By measuring the energy change of the backscattered projectiles at a certain angle, information on the nature and concentration of the target atoms as well their depth distributions can be obtained [10]. In this investigation, the helium ($^1\text{He}^+$) ions of energy 1.4 MeV were used as projectiles for studying the interface reactions between ruthenium and 6H-SiC. Raman spectroscopy was also used to analyse the thin film sample which was annealed at 1000 °C. Both of these measurements were done at room temperature. The Schottky diodes were analysed by current-voltage (IV) and capacitance-voltage (CV) characterisation at an ambient temperature of 24°C after each annealing process using a 4140B PA meter /DC voltage source by Hewlett Packard, which was interfaced to a LabVIEW-operated computer. The CV measurements were done at a frequency of 1MHz, and the maximum reverse voltage was -2 V. Both the IV and CV measurement data were automatically saved on the computer by LabVIEW.

3. Results and Discussion.

RBS data was simulated using RUMP software[11]. RUMP is a computer code which requires user entry to fit the raw RBS spectra. This fitting, otherwise known as simulations, gives layer by layer information about the film thickness and composition. The composition and thickness of the deposited film and reaction layers can then be

converted to depth profiles. The red plots in Fig. 1 to Fig.4 are the RUMP simulated plots while the black plots are the raw RBS spectra.

From RBS analysis it is observed that the as-deposited RBS spectrum of Ru-6H-SiC (not shown) is similar to the sample annealed at 500 °C in a vacuum (Fig. 1). There is indication of Ru_2Si_3 formation at 600 °C as evidenced by the presence of a step near the high energy step of Si (Fig.2). The silicide formation is more pronounced at annealing temperature of 1000 °C as indicated by steps on the high energy edge of Si and low energy edge of Ru (Fig. 4). Diffusion of Ru into SiC commences at 800 °C (not shown), and is more pronounced at 900 °C as indicated by a very wide bottom of Ru signal (Fig.3). Plots of depth profiles (Fig.5 and Fig. 6) have been obtained from RUMP simulations. From these simulations, it is observed that Ru diffuses into 6H-SiC, and the dissociated Si and C atoms also diffuse into Ru. The reaction zone increases with annealing temperature. The Ru/6H-SiC interface of the as-deposited sample (Fig.5) is located 320×10^{15} at./ cm^2 from the surface of Ru. Ru is observed to react with 6H-SiC, and is found at 2300×10^{15} at./ cm^2 from the surface (Fig.6) after annealing at 1000°C.

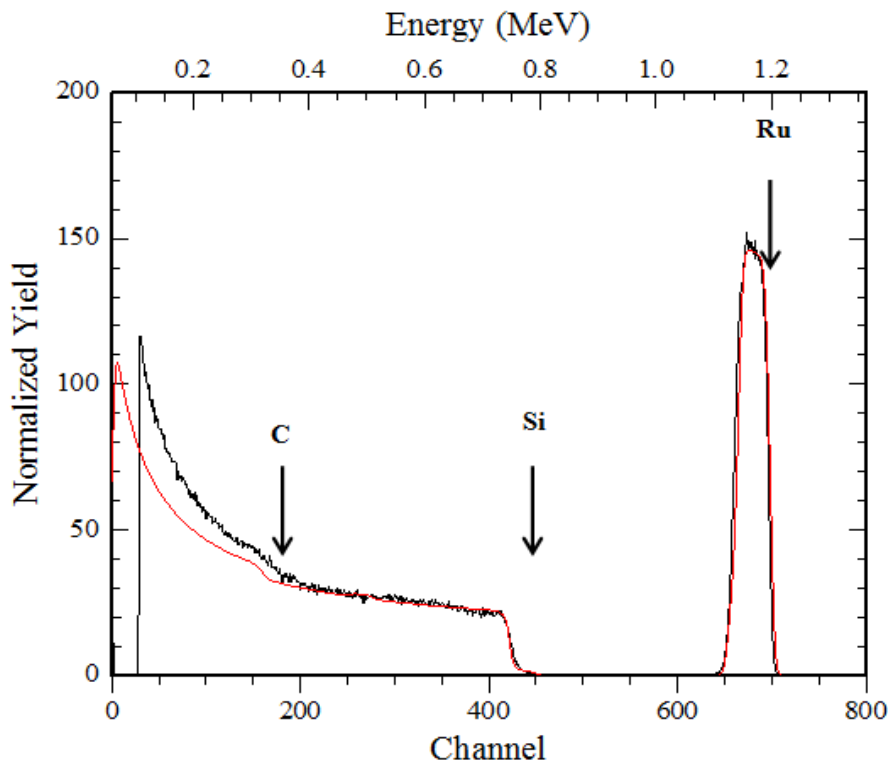


Fig. 1. RBS spectra of Ru-6H-SiC annealed in a vacuum at 500°C obtained by using 1.4 MeV of helium ions. The black and red plots are actual and simulated profiles respectively.

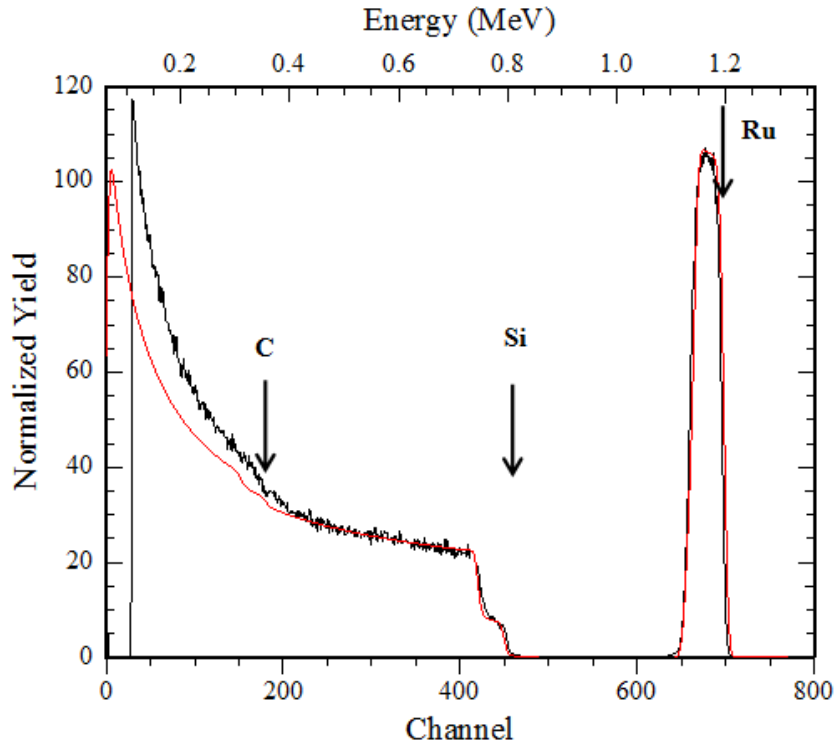


Fig. 2. RBS spectra of Ru-6H-SiC annealed in a vacuum at 600°C obtained by using 1.4 MeV of helium ions. The black and red plots are actual and simulated profiles respectively.

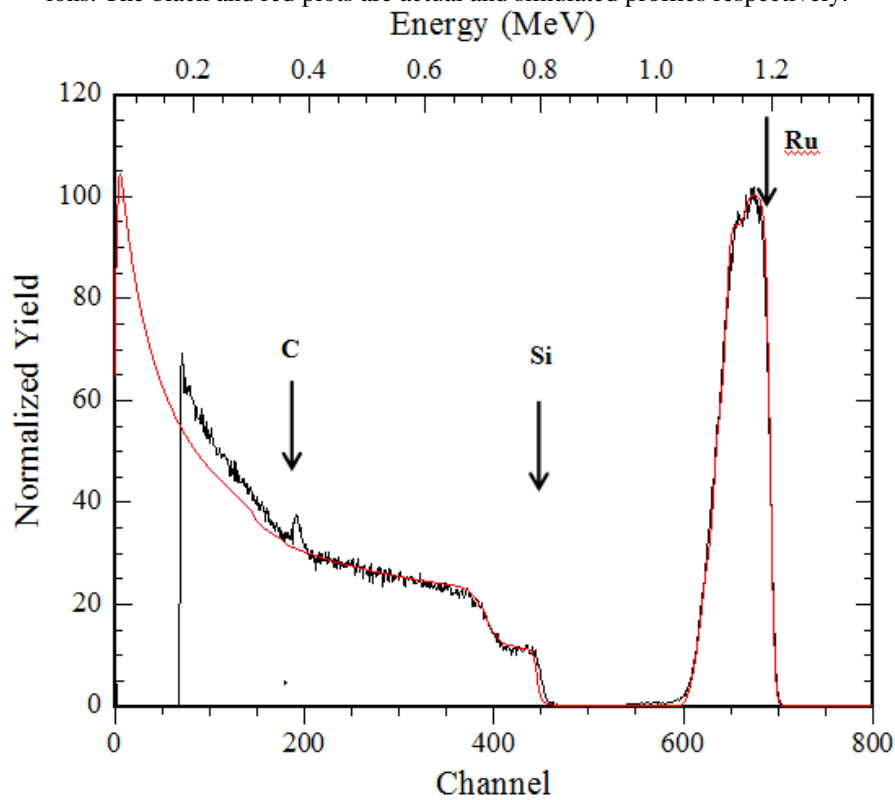


Fig. 3. RBS spectra of Ru-6H-SiC annealed in a vacuum at 900°C obtained by using 1.4 MeV of helium ions. The black and red plots are actual and simulated profiles respectively.

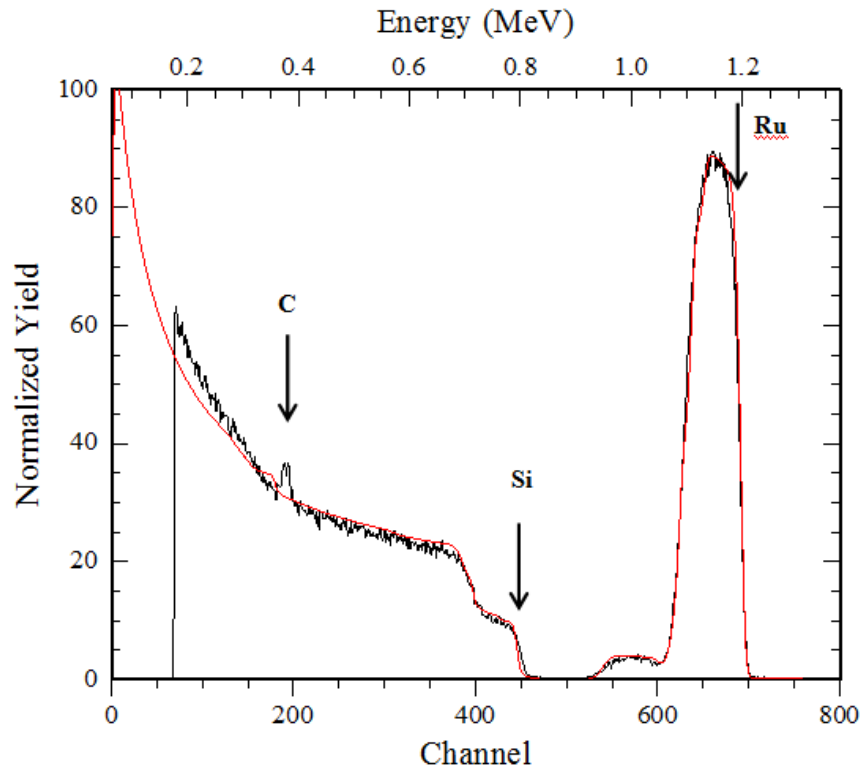


Fig. 4. RBS spectra of Ru-6H-SiC annealed in a vacuum at 1000°C obtained by using 1.4 MeV of helium ions. The black and red plots are actual and simulated profiles respectively.

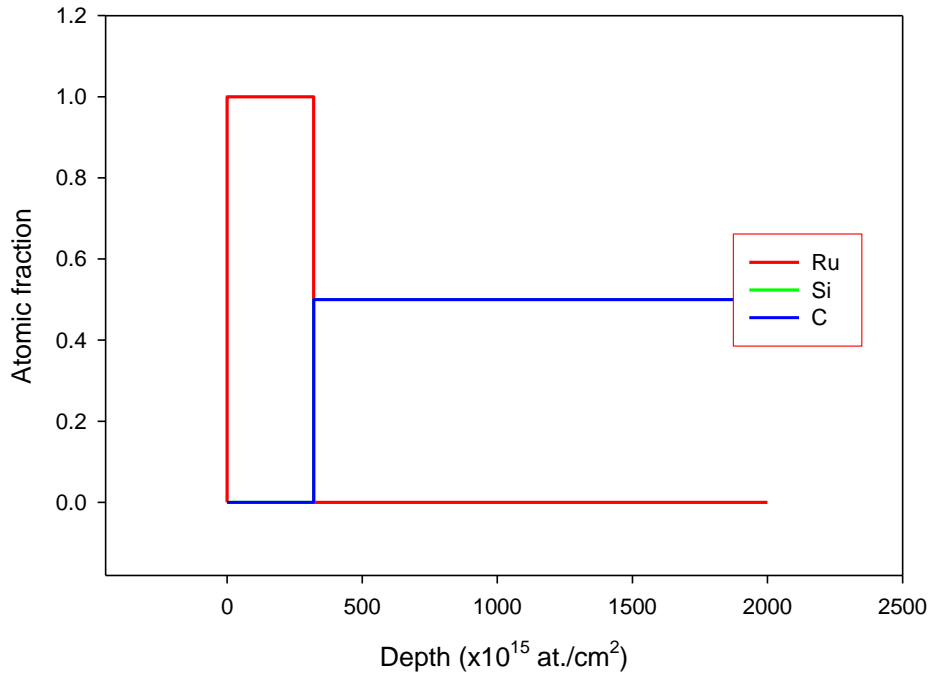


Fig. 5. Depth profile of as-deposited Ru-6H-SiC

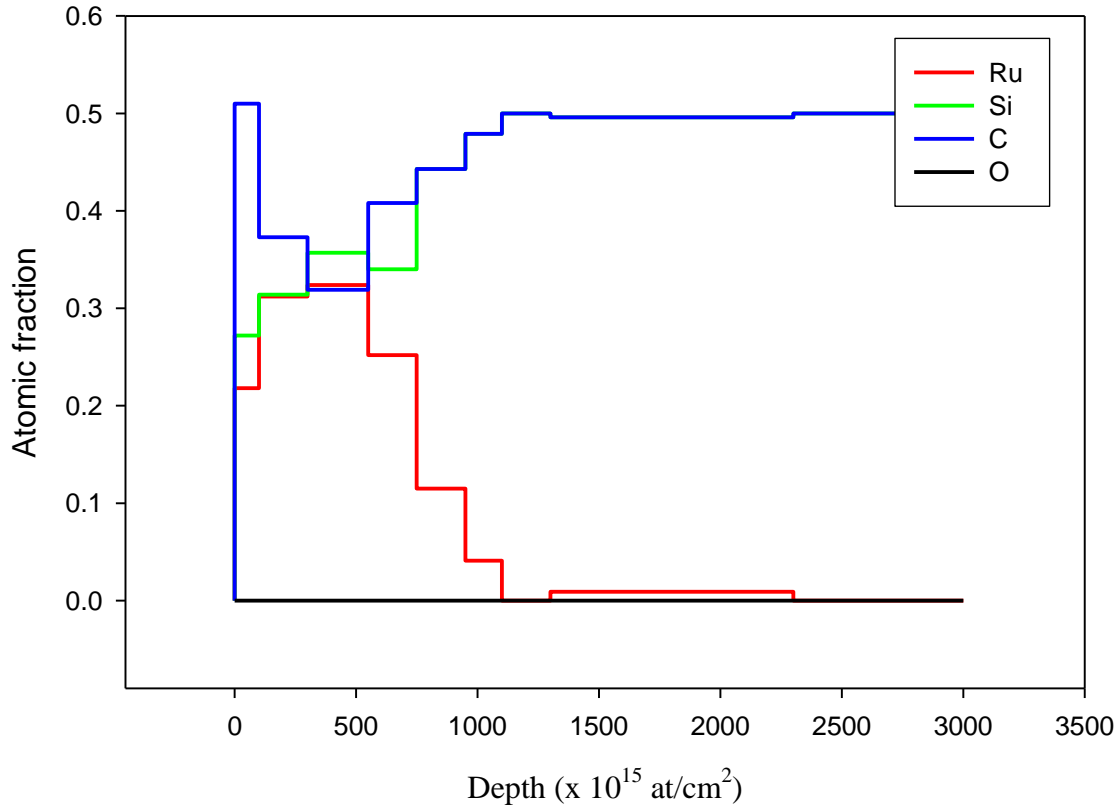


Fig. 6. Depth profile of Ru-6H-SiC annealed at 1000 °C in a vacuum.

Raman analysis of the thin film sample (Fig. 7) shows the formation of graphite as indicated by a typical carbon D peak at 1354 cm^{-1} and G peak at 1589 cm^{-1} [12,13,14,15,16,17]. The intensity ratio of the D and G peak are used to approximate the size of the crystalline graphite or degree of disorder of the graphite. The D band is generally thought to be an indication of disordered or defective hexagonal planar graphite structures [12]. The G band originates from the stretching vibrations in the basal plane of ideal graphite, and a combination of D and G bands is generally regarded as an indication of polycrystalline graphitic structures [13]. According to Lu et al [13] the absence of a broad amorphous carbon peak at position 1510 cm^{-1} in the Raman spectrum is an indication of the absence of this type of carbon in the sample. There is also an indication from Raman analysis of the formation of Ru_2Si_3 as evidenced by the appearance of the peak immediately left of 300 cm^{-1} position [18]. This silicide formation is corroborated by RBS analysis of the sample.

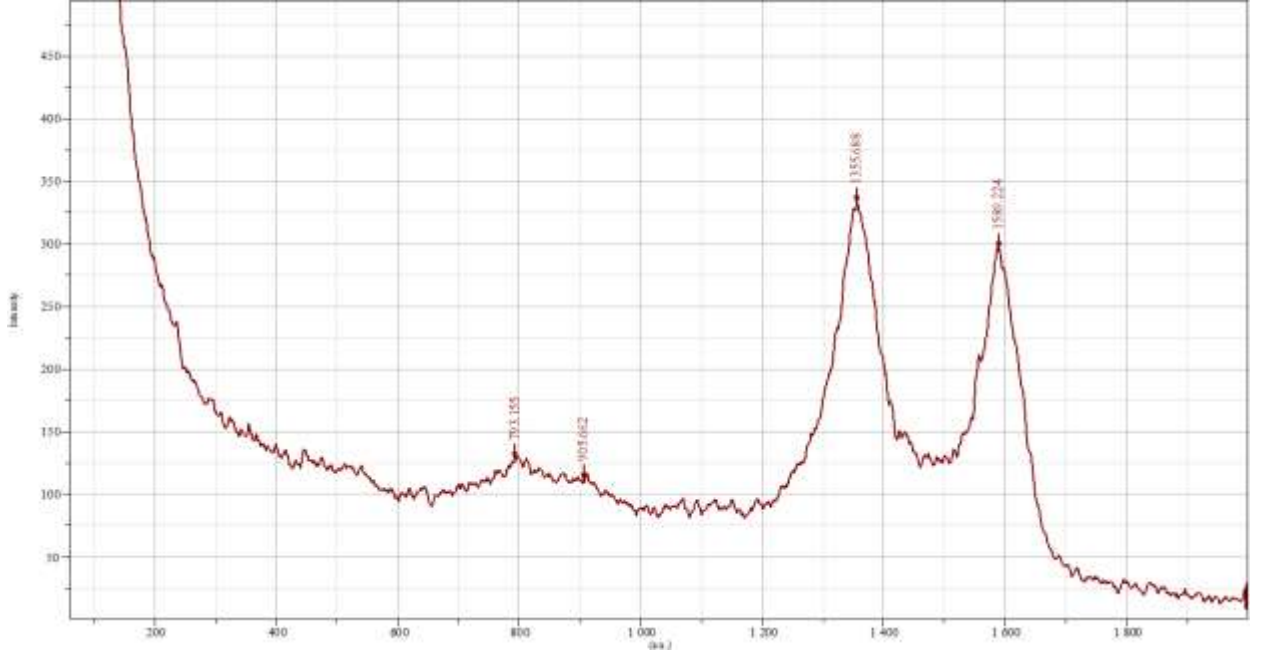


Fig. 7. Raman spectrum of Ru-6H-SiC film annealed in vacuum at 1000 °C .

The Ru-6H-SiC Schottky diodes were evaluated using IV and CV characteristics. The IV characteristics were used on the assumption that current transport through the diode is by thermionic emission. Majority carriers are mainly responsible for current transport in a schottky junction . For schottky barrier diodes operated around room temperature, thermionic emission is the dominant transport mechanism of majority carriers from the semiconductor into the metal. An electron can be thermionically emitted from the semiconductor surface into the metal if it has an energy which is greater than the barrier height [19]. The SBH, ϕ_{Bn} , ideality factor, η , and reverse saturation current, I_S , were obtained from IV characteristics by assuming that the Schottky diodes obey the thermionic emission current transport model [19] given by equation

$$J = J_s (e^{\frac{qV}{\eta kT}} - 1) \quad \text{where } J_s = A^* T^2 e^{-\frac{q\phi_{Bn}}{kT}} .$$

J_s is the reverse saturation current density , T is absolute temperature in Kelvin, k is the Boltzmann constant, q is the absolute amount of charge on an electron, and A^* is the Richardson constant which is equal to $72 \text{ Acm}^{-2}\text{K}^{-2}$ for 6H-SiC [20]. It should be noted that a proper determination of the Richardson constant can be done by performing a “conventional”

Richardson plot [21]. This is basically a plot of $\ln\left(\frac{I_s}{T^2}\right)$ vs $\frac{1}{kT}$ where the natural log intercept will provide the product SA^* . S in this case is the area of the diode. However this was not performed due to the limitation of the equipment. To get this data one needs to anneal and extract electrical data simultaneously.

Series resistance R_S is the resistance of the bulk material of the semiconductor plus that of the back ohmic contact, and to account for the series resistance, the current equation is modified [19]

$$\text{to become } J = J_s \left[e^{\frac{q(V-IR_S)}{\eta kT}} - 1 \right] .$$

The CV technique uses the fact that the width of the reverse-biased depletion region of a metal semiconductor junction varies with the applied voltage. Using this technique the parameters of the SBD are obtained from the junction capacitance equation of the SBD [19] which is given by

$$C = \sqrt{\frac{q\epsilon_s N_D}{2(V_{bi}-V)}} . \text{ Re-arranging this equation}$$

gives $\frac{1}{C^2} = \frac{2(V_{bi}-V)}{q\epsilon_s N_D} (\text{Fcm}^{-2})^{-2}$. Where C is the capacitance per unit area, V_{bi} is the

built in potential, V is the biasing voltage, ϵ_s is the dielectric constant of 6H-SiC, q is the charge on an electron and N_D is the donor doping density.

A plot of $\frac{1}{C^2}$ versus V will give a straight line, and a donor doping density N_D can be extracted from the graph. The SBH is determined from the voltage intercept [19] by the equation

$$\phi_{Bn} = V_i + V_o, \text{ where } V_i \text{ is the voltage intercept, and } V_o = \frac{kT}{q} \ln\left(\frac{N_C}{N_D}\right).$$

N_C is the effective density of states in the conduction band of 6H-SiC. N_C is equal to $8.9 \times 10^{19} \text{cm}^{-3}$ for 6H-SiC at 300 K [20].

Table 1 contains the diodes parameters that were extracted from CV and IV characteristics. From the table, it is observed that the ideality factor generally decreases with annealing temperature whereas there is little variation of SBH obtained by IV characteristics. A plot of the CV characteristics (Fig.8) indicates that the SBDs are stable up to annealing temperature of 700 °C, and above this temperature the performance of the SBH deteriorates as evidenced by the non-linearity of the CV characteristic . For the sample annealed at a temperature of 900 °C , the CV data is scattered all over the graph thereby making it impossible to produce a plot. This behaviour pattern was repeated from one sample to another. The deterioration of the electrical performance of the SBD may be attributed to the diffusion of Ru into 6H-SiC. The formation of Ru_2Si_3 at temperatures of 800°C cannot be the cause on its own for the worsening of the performance of the Schottky diode as the silicide is semiconducting, and has a barrier height close to that of Ru. The SBH of Ru_2Si_3 on silicon (which one can conjecture to be close to that on SiC) of 0.76 eV [22] is very close to the SBH of Ru on SiC. It is the carbon released during the reaction process that may be the cause of poor performance of the diode. IV plots however indicate that the SBD malfunctions only after annealing at 900 °C. This difference in indication of the performance degradation temperature between IV and CV characteristics might be due to

the availability of interface states or traps [23,24]. These are localised electronic states in the bulk of a semiconductor. Interface states affect CV characteristics (more than IV characteristics) by bending the C^2 -V plots [24] as indicated by the 800 °C plot in Fig. 8 . According to Perret [23] interface states have been shown to increase with increasing temperature (especially at temperatures of more than 600 °C) in an inert annealing environment.

From the plot of IV characteristics (Fig.9), it is also observed that the forward voltage drop V_F generally decreases with higher annealing temperatures. This electrical behaviour can be explained with the help of the equation of the forward voltage drop of the Schottky diode [25] which is obtained from the thermionic current transport equation above by simply making the forward voltage the subject of the formula:

$$V_F = \frac{\eta kT}{q} \ln\left(\frac{J_F}{A^* T^2}\right) + \eta\phi_{Bn} + R_{on,sp} J_F \quad (1)$$

Where J_F is the forward current density, and $R_{on,sp}$ is the specific on resistance which is equal to the sum of series resistance of a substrate and drift region [26]. The authors wish to point out that the electrical data were obtained at room temperature but there are plans to procure *in situ* measuring apparatus. This apparatus will enable the simultaneous extraction of electrical data during the annealing process. From Table 1, it can be observed that there is a general decrease of series resistance with annealing temperature. The decrease in series resistance may be attributed to the increase in ionization of the donor atoms at high annealing temperatures [25]. The other reason may be that the contact becomes more intimate with the substrate as the annealing temperature is increased. It is also observed from the table that fluctuations of SBH (obtained from IV characteristics) at various annealing temperatures are very small. From these data and equation (1), the forward voltage drop of the Schottky diodes should be expected to decrease with increasing annealing temperature. This is aptly demonstrated by the IV characteristics of the SBDs in Fig.9.

Another observation that can be made from Table 1 is that the SBHs which are obtained from CV characteristics are higher than those obtained from IV characteristics. Normally the SBHs that are obtained from CV measurements are slightly higher than those from IV characteristics. These differences may be due to the presence of inhomogeneous interfaces, which result in non-uniform Schottky contacts where current can flow via two pathways (i.e. over a lower barrier or a higher barrier) [27]. IV characteristics are more sensitive to small regions with low SBH than CV characteristics [28]. Guy *et al* [29] have argued that the difference in SBH measured by the two methods is due to the presence of an additional capacitance at the metal-semiconductor interface which originates from a thin oxide layer which comes as a result of surface preparation. The general increase with annealing temperature of the SBH obtained from CV characteristics might be attributed to microstructure transformation of the Ru-6H-SiC interface as evidenced by RBS and Raman analysis above.

The SBDs become ohmic after annealing at 900 °C as evidenced by a best fit IV line which passes through the origin (Fig. 9) . The ohmic behaviour exhibited by the Ru-6H-SiC SBDs at this annealing temperature may be attributed to the formation of graphite at the metal-SiC interface as confirmed by Raman analysis . This finding is supported by Seyller *et al* [30] who in their studies found that the formation of graphite at the metal-SiC interface may lead to ohmic contact formation as the SBH of graphite on n-type 6H-SiC is very small (about 0.3 eV) . Lu *et al* [13] also found out that the carbon contact on SiC exhibited schottky and ohmic contact behaviour in the annealing temperature range of 900-1350 °C. They found that the temperature of transition from schottky to ohmic contact in Carbon/SiC structure depends on the doping concentration of SiC and amount of nano-graphitic flakes formed.

Annealing Temp	Ideality η	SBH From IV (eV)	SBH From CV (eV)	Series Resistance R_s (Ω)	Saturation Current I_s (A)	Donor Density N_D (cm^{-3})
As dep	3.511	0.493	0.600	31.487	7.612E-5	2.337E+18
500°C	2.845	0.532	1.701	25.196	1.709E-5	7.845E+18
600°C	1.962	0.536	1.256	16.088	1.43E-05	5.25E+18
700°C	1.271	0.494	1.727	20.451	7.53E-05	3.28E+18
800°C	1.296	0.533	*	11.839	1.65E-05	*
900°C	1.472	0.419	**	4.598	1.41E-03	**

*CV curve is not a straight line.

** CV data is scattered all over the graph area.

Table 1. Parameters of Ru-6H-SiC schottky diodes at various vacuum annealing temperatures

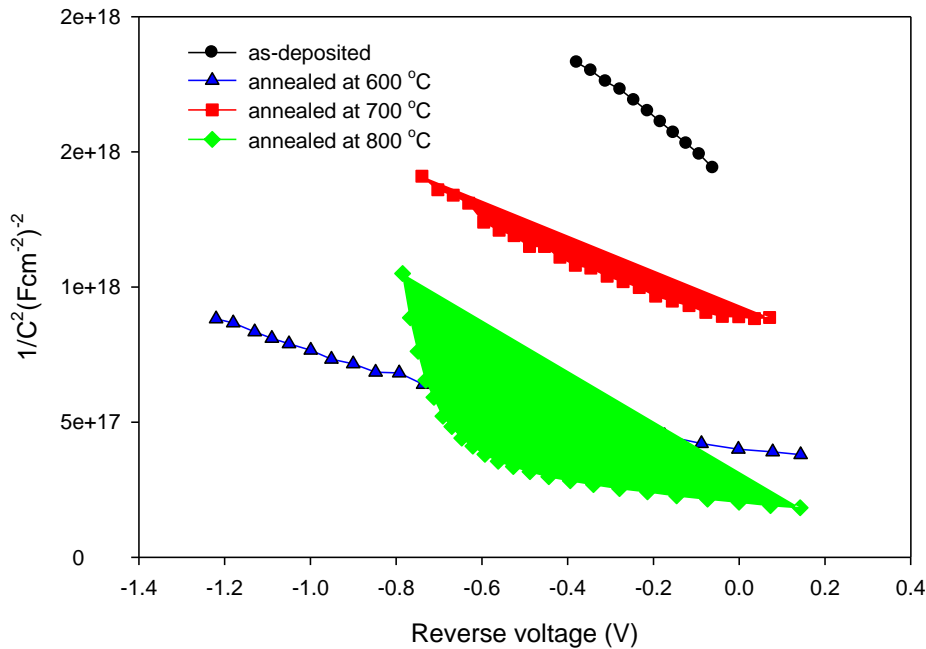


Fig. 8. CV characteristics obtained at room temperature of Ru-6H-SiC annealed in a vacuum.

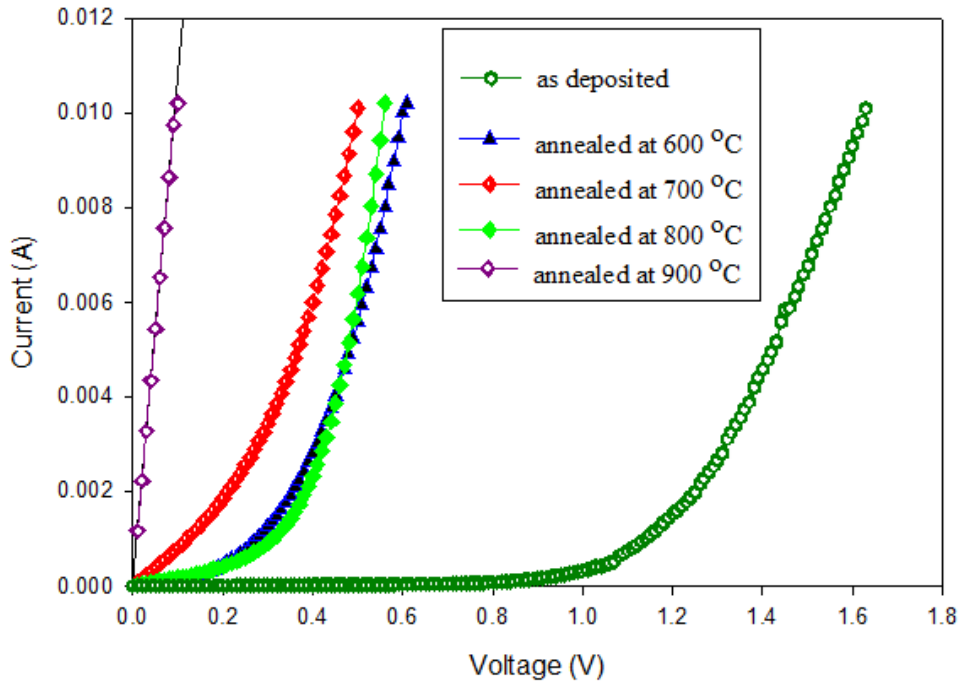


Fig. 9. IV characteristics obtained at room temperature of Ru-6H-SiC annealed in a vacuum.

4. Conclusion

This study has shown that the Ru-6H-SiC SBDs annealed in a vacuum remain operational up to an annealing temperature of 700 °C, and degrade above this temperature. The degradation of the Schottky diode is explained by the fact that the schottky contact becomes ohmic due to the formation of graphite . The formation of graphite results from Ru_2Si_3 formation. The diffusion of Ru into the SiC layer might be another reason for the poor performance of the diode after annealing temperature of 700 °C. Both Ru diffusion and silicide formation have been confirmed by RBS analysis and Raman spectroscopy.

5. References

- [1] L. Stuchlikova, D. Buc, L. Harmatha, U. Helmerson, W. H. Chang, I. Bello, *Deep energy levels in RuO₂/4H-SiC Schottky barrier structures*, Applied Physics Letters **88**, 153509 (2006).
- [2] D. Buc , L. Stuchlikova , U. Helmerson , W.H. Chang.,I. Bello I, *Investigation of RuO₂/4H-SiC Schottky diode contacts by deep level transient spectroscopy*, Chemical Physics Letters **429** 617–621 (2006).

- [3] K.V. Munthali, C. Theron, F.D. Auret, S.M.M. Coelho, E. Njoroge, L. Prinsloo, *Solid state reaction of ruthenium with silicon carbide, and the implications for its use as a Schottky contact for high temperature operating Schottky diodes*, Material Science and Engineering B (2013).
- [4] L. Stuchlikova, D. Buc, L. Harmatha, U. Helmersson, W. H. Chang, I. Bello, *Deep energy levels in RuO₂/4H–SiC Schottky barrier structures*, Applied Physics Letters **88**, 153509 (2006).
- [5] D. Buc, L. Stuchlikova, U. Helmersson, W.H. Chang, I. Bello, *Investigation of RuO₂/4H–SiC Schottky diode contacts by deep level transient spectroscopy*, Chemical Physics Letters **429** 617–621 (2006).
- [6] D. Buc, L. Stuchlikova, L. Harmatha, I. Hotovy, *Electrical characterization of 4H–SiC Schottky diodes with a RuO₂ and a RuWO_x Schottky contacts*, J Mater Sci: Mater Electron **19**:783–787 (2008).
- [7] S. Roy, C. Jacob, M.Zhang, S. Wang, A.K. Tyagi, S. Basu, *SIMS, RBS and glancing incidence X-ray diffraction studies of thermally annealed Ru/β-SiC interfaces*, Applied Surface Science **211** 300–307 (2003).
- [8] A. Venter, M.E.Samiji, A.W.R.Leitch, *Thermal stability of Ru, Pd and Al Schottky contacts to p-type 6H-SiC*, phys. stat. sol. (c) **1**, No. 9, 2264–2268 (2004).
- [9] E. Stuchlikova, L. Harmatha, D. Buic, J. Benkowska, B. Hlinka, G. G. Siu, *4H-SiC Diode with a RuOX and a RuWO_x Schottky Contact Irradiated by Fast Electrons*, IEEE. (2006).
- [10] W. Chu, J.W. Mayer, M.A. Nicolet, *Backscattering Spectrometry*, Academic Press Inc (1978).
- [11] L.R. Dolittle, *Algorithms for the rapid simulation of Rutherford backscattering spectra*, Nuclear Instruments and Methods B9, 344, (1985).
- [12] Zhen-Yu Juang, Chih-Yu Wu, Chien-Wei Lo, Wei-Yu Chen, Chih-Fang Huang, Jenn-Chang Hwang, Fu-Rong Chen, Keh-Chyang Leou, Chuen-Horng Tsai, *Synthesis of graphene on silicon carbide substrates at low temperature*, Carbon vol 47, 2026–2031,(2009).
- [13] W. Lu, W.C. Mitchel, C.A. Thornton, G.R. Landis, W.E. Collins, *Carbon Structural Transitions and ohmic contacts on 4H-SiC*, Journal of Electronic Materials, Vol. 32, No. 5 (2003).
- [14] C. Faugeras, A. Nerrière, M. Potemski, A. Mahmood, E. Dujardin, C. Berger, W. A. de Heer, *Few-layer graphene on SiC, pyrolytic graphite, and graphene: A Raman scattering study*, Applied Physics Letters **92**, 011914 (2008).
- [15] V. Mennella, G. Monaco, L. Colangeli, E. Bussolletti, *Raman spectra of carbon-based materials excited at 1064 nm*, Carbon vol 33, No. 2, pp 115-121, (1995).
- [16] H. Hiura, T.W. Ebbesen, K. Tanigaki, *Raman studies of carbon nanotubes*, Chemical Physics Letters vol 202, number 6, (1993).
- [17] P.C. Eklund, J.M. Holden, R.A. JISHI, *Vibrational modes of carbon nanotubes; Spectroscopy and Theory*, Carbon vol. 33, No. 7 pp. 959-972, (1995).
- [18] Jelenkovic E.V, Tong K .Y, Cheung W. Y, Wong S. P, 2003, *Physical and electrical properties of sputtered Ru₂Si₃/Si structures*, Semiconductor Science Technology 18, 454-459.
- [19] S.M. Sze, *Semiconductor Devices Physics Technology*, 2nd edn. (John Wiley & Sons, New York), pp.47-127(2002)
- [20] <http://www.ioffe.rssi.ru/SVA/NSM/Semicond/SiC/bandstr.html>, accessed on 25 April 2013.
- [21] Roccaforte, F. La Via, F. A. Makhtari, V. Raineri, R Pierobon, L. E. Zanoni, *Richardson's Constant in inhomogeneous silicon carbide Schottky contacts*, Journal of Applied Physics, vol. 93, No. 11, (2003).

- [22] E.V. Jelenkovic, K.Y. Tong, W.Y. Cheung, S.P. Wong, *Semicond. Sci.Technol.* 18, 454-459 (2003).
- [23] R.F. Pierret, *Semiconductor Device Fundamentals*, (Addison-Wesley, Massachussets), pp.661-667 (1996).
- [24] A. Tataroglu, S. Altindal, *Characterisation of current-voltage (I-V) and capacitance-voltage-frequency (C-V-f) features of Al/SiO₂/p-Si (MIS) Schottky diodes*, *Microelectronic Engineering* 83, 582-588, (2006).
- [25] R. Raghunathan, D. Alok , B.J. Baliga, *High Voltage 4H-SiC Schottky Barrier Diodes*, *IEEE Electron Device Letters*, Vol. 16. No. 6.
- [26] A. Itoh, T. Kimoto, H. Matsunami, *Efficient Power Schottky Rectifiers of 4H-SiC*, *Proceedings of 1995 International Symposium on Power Semiconductor Devices and ICs*.
- [27] F. La Via, F. Roccaforte, A. Makhtari, V. Raineri, P. Musumeci, L. Calcagno, *Structural and electrical characterisation of titanium and nickel silicide contacts on silicon carbide*, *Micro-electronic Engineering* 60 269–282, (2002).
- [28] H.-J. Im, B. Kaczer, J.P. Pelz, S. Limpijumnong , W.R.L. Lambrecht, and W.J. Choyke, *Nanometer-Scale Investigation of Metal-SiC Interfaces Using Ballistic Electron Emission Microscopy*, *Journal of Electronic Materials*, Vol. 27, No. 4, (1998).
- [29] J. Guy, M. Lodzinski, A. Castaing, P.M. Igit, A. Perez-Tomas, M.R. Jennings, P.A. Mawby, *Silicon carbide Schottky diodes and MOSFETS: solutions to performance problems*, 2008 13th International Power Electronics and Motion Control Conference.
- [30] T. Seyller, K.V. Emtsev, F. Speck, K.Y. Gao, L. Ley, *Schottky barrier between 6H-SiC and graphite: Implications for metal/SiC contact formation*, *Applied Physics Letters* 88, 242103 (2006).